



HAL
open science

Numerically Simulated Comparison of RF Frequencies Generation by Up-conversion using Photonic Mixing in Semiconductor Optical Amplifiers

Filipe L. T. da Silva, Ricardo M. Ribeiro, Bárbara Dumas Feris, Thierry Rampone, Ammar Sharaiha

► **To cite this version:**

Filipe L. T. da Silva, Ricardo M. Ribeiro, Bárbara Dumas Feris, Thierry Rampone, Ammar Sharaiha. Numerically Simulated Comparison of RF Frequencies Generation by Up-conversion using Photonic Mixing in Semiconductor Optical Amplifiers. XLI BRAZILIAN SYMPOSIUM ON TELECOMMUNICATIONS AND SIGNAL PROCESSING - SBrT 2023, Oct 2023, São José dos Campos, Brazil. hal-04703212

HAL Id: hal-04703212

<https://hal.science/hal-04703212v1>

Submitted on 19 Sep 2024

HAL is a multi-disciplinary open access archive for the deposit and dissemination of scientific research documents, whether they are published or not. The documents may come from teaching and research institutions in France or abroad, or from public or private research centers.

L'archive ouverte pluridisciplinaire **HAL**, est destinée au dépôt et à la diffusion de documents scientifiques de niveau recherche, publiés ou non, émanant des établissements d'enseignement et de recherche français ou étrangers, des laboratoires publics ou privés.

Numerically Simulated Comparison of RF Frequencies Generation by Up-conversion using Photonic Mixing in Semiconductor Optical Amplifiers

Filipe L. T. da Silva, Ricardo M. Ribeiro, Bárbara D. Feris, Thierry Rampone and Ammar Sharaiha

Abstract—In order to perform photonic mixing and Radio Frequency (RF) generation by frequency up-conversion, the authors analyze the use of a single Semiconductor Optical Amplifier (SOA) and a Semiconductor Optical Amplifier-Mach-Zehnder Interferometer (SOA-MZI) structure by computer simulation using Advanced Design System (ADS) software. It assesses and compare both devices in terms of RF conversion gain and Cross Gain Modulation/Cross Phase Modulation (XGM/XPM) bandwidth. The simulations were carried out as function of several bias currents by mixing one and two optical input signals. Results have shown that SOA-MZI presents an average RF conversion gain 1 dB higher than single SOA.

Keywords—Cross-gain modulation; Cross-phase modulation; Photonic mixing; Semiconductor optical amplifier; Up-conversion frequency.

I. INTRODUCTION

The ever growing demand for total data traffic capacity has been requiring continuous advancing in optical fiber communication networks technology over the past twenty-five years [1]-[3]. This can be possible partially due to the development of new optoelectronic devices and technologies such as Microwave Photonics (MWP). The latter combines the radiofrequency and optoelectronics [4].

Optical Amplifiers (OAs) are a key device in MWP and can be divided in two classes: Optical Fiber Amplifiers (OFAs) and Semiconductor Optical Amplifiers (SOAs) [1]. Since OAs are intrinsically broadband devices, it becomes crucial to overcome issues (signal attenuation, dispersion, crosstalk, etc...) of radio-over-fiber systems and Wavelength Division Multiplexing (WDM) networks [2],[3].

SOAs are fed by electrical (bias) current. They have an active layer in which the optical signal is transmitted in both forward and backward directions. SOAs are originally and mostly used for unidirectional or bidirectional optical gain. However, many researches have been carried out along the years exploiting other functions of SOAs that are difficult or impossible to implement with electronics or other types of OAs: wavelength conversion by using the four-wave mixing

(FWM) – a coherent nonlinear process – [5], multiplexing/demultiplexing [6], switching [7], etc.

In MWP, the frequency up-conversion is a nonlinear process [8] where the lower RF frequency of a modulated signal is translated to a higher frequency optical signal by keeping its characteristics by means the photonic mixing. RF frequency conversion based on photonic mixing are of great interest on processing, analyzing and detections of signals in the radio-over-fiber systems and many optical setups [9].

In spite of the fact that the ADS software has been designed in many applications, mainly in electrical/electronic schemes, here it has been adapted to perform in photonic simulations. This is enabled due to an existing model developed in [10] called Time-Domain Transfer Matrix Model (TDTMM). The TDTMM can be used to study complex modulation formats since it can precisely handle with both phase and amplitude of light signals. This model can be considered as an equivalent circuit allowing to extract powers in optical domain due to the electro-optical conversion. The TDTMM can simultaneously describe the evolution of light signals, Amplified Spontaneous Emission (ASE) and the carrier density.

Firstly, it will be shown the simulations of the: gain and frequency response for a single optical input power and the XGM/XPM Bandwidth (BW) for two optical signals (probe Continuous Wave (CW) + pump modulated at Local Oscillator (LO) frequency) for a single SOA system. In a second step, this work presents the simulation results of a SOA-MZI scheme to observe the: system phase, output optical powers as function of pump (control) power, XGM/XPM bandwidth and up-converted RF gain by mixing of two optical input signals with wavelengths of 1540 nm and 1550 nm. Furthermore, the main contribution is the comparison of the XGM/XPM bandwidth and the converted RF gain between single SOA and SOA-MZI.

The paper is organized as follows. In Section II, the theoretical model for SOA-based devices and the implementation using ADS are presented. In section III, a single SOA system is described by launching one and two input signals. In section IV, the SOA-MZI device is explained and their simulation results are presented. In section V, it is shown the comparison between single SOA and SOA-MZI device. Finally, in section VI conclusions are outlined.

II. THEORETICAL MODEL FOR SOA-BASED DEVICES

TDTMM is a generalized time-domain approach allowing an easier development and implementation of physical problems [10]. The model used for simulations is bi-directional, i.e. both for signals and ASE can be cascaded. Therefore, it enables complex optical system simulations [11]-[13] in both direction of propagation. In addition, it is also a field-based rate equation model, that is, it allows to deal with complex modulations as Binary Phase Shifting Key (BPSK), Quadrature Phase Shift Keying (QPSK), Quadrature Amplitude Modulation (QAM) and Frequency-Shift Keying (FSK) which can handle with a very high bit rate modulations.

The SOA model can be represented as an equivalent circuit as shown in Fig. 1, which is important for the use of ADS to simulate many types of calculations (DC, AC, Transient, Harmonic Balance, etc.).

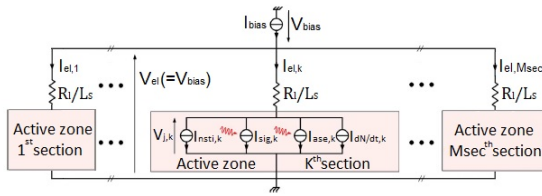


Fig. 1. ADS equivalent circuit of the SOA model [10].

Fig. 1 presents a model that allows to calculate the carrier density from the current and voltage applied to the SOA. The active layer of the SOA is divided in k sections along its length because the carrier density drops with the voltage due to the bias current as shown in equation (1):

$$\ln\left(\frac{N_k}{N_e}\right) = \frac{V_{el} - \frac{R_l}{L_s} I_{el,k}}{\eta \frac{K_B T}{q_e}} \quad (1)$$

Where V_{el} is the bias voltage applied and $I_{el,k}$ the bias current at k sections.

The TDTMM model has been validated in static (gain and noise figure), slow and fast dynamic (gain recovery time in a pump-probe configuration) regimes. According to the simulation model, the gain has reached 0.5 dB of average error [10].

III. THE SINGLE SOA DEVICE

In this section, first, simulation results of the gain as a function of wavelength and input optical power are presented. Subsequently, the frequency response for a single input optical signal is introduced. The last, but not least, a description of how the XGM/XPM BW and the conversion gain (CG) was numerically simulated for two input optical signals is carried out.

A. Single input optical signal

For the first simulation, the ADS scheme for a single SOA is given by Fig. 2.

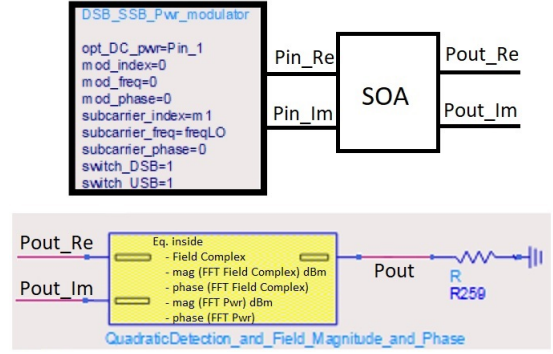


Fig. 2. The single SOA ADS circuit.

The box on the top represents a circuit in a low hierarchy that works as a double-sideband (DSB) modulator which has embedded the input power (P_{in}), wavelength (λ), RF frequency modulation ($freq_{LO}$) and modulation index (m). I_{BIAS} is the bias current and P_{out} is the output power. Since the results that can be produced by the circuit of Fig. 2 are given by electrical fields with real and imaginary parts, the yellow box on the bottom becomes necessary to convert electrical fields to optical powers by means of quadratic detection.

DC simulations have provided the amplification gain as a function of wavelengths and input powers as showed in Fig. 3 and Fig. 4, respectively. The frequency response is shown in Fig. 5. For the simulations, it is used four bias current values: 0.125, 0.25, 0.375 and 0.5 A.

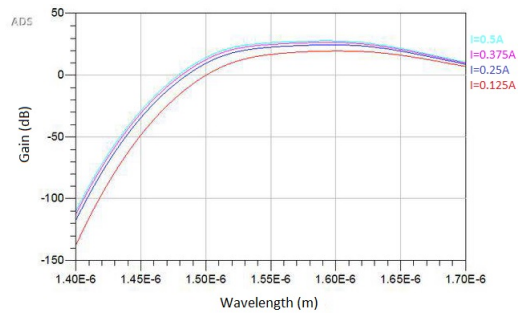


Fig. 3. Amplification gain as function of wavelength, for several bias current values at a fixed input power of -10dBm.

To observe the peak gain, results were chosen for $I_{BIAS} = 0.5$ A. Therefore, for $P_{in} = -10$ dBm, -20 dBm and -30 dBm, the peak gain occurred at 27.7 dB at 1592 nm, at 31.5 dB at 1575 nm and at 32 dB at 1573 nm, respectively.

From the graphic shown in Fig. 4, it can be observed the saturation effect, i.e. when the maximum input optical power drops 3 dB. It means that, for 1574 nm (around the highest peak gain in Fig. 3), the saturation power reached around -12 dBm for every bias current value.

An AC simulation sequence has been done to obtain the frequency response of the single SOA. Fig. 5 shows the gain in terms of frequency.

Fig. 5 presents the frequency response for the input optical signal of -10 dBm at wavelength of 1550 nm. For both low

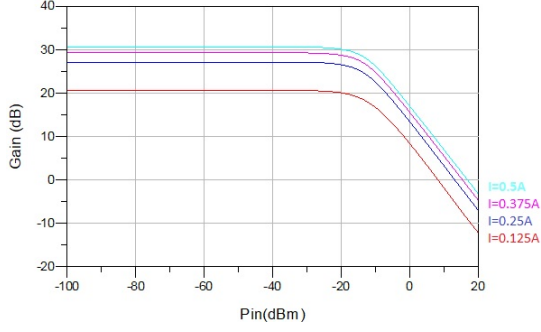


Fig. 4. Amplification gain as function of input optical power, for several bias current values at a fixed wavelength of 1574 nm.

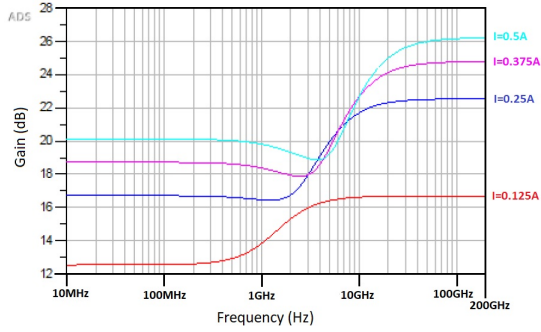


Fig. 5. Frequency response for several bias current, for a fixed input power of -10 dBm at wavelength of 1550 nm.

and high frequencies, the gain is constant. Non-linear effects can be observed from 1 to 5 GHz at higher bias current. The equation (2) can explain this behavior shown in Fig. 5.

$$|\Delta p_{out}| = \Delta p_{in} \bar{G} \frac{(1 + K_T)}{(1 + K_T \bar{G})} \sqrt{\frac{1 + \left(\frac{\omega \tau}{1 + K_T}\right)^2}{1 + \left(\frac{\omega \tau}{1 + K_T \bar{G}}\right)^2}} \quad (2)$$

Where $K_T = \bar{P}_{in}/P_{sat}$ is the ratio between the average input optical power and saturation power. $\bar{G} = (\delta G/\delta N)\Gamma\alpha_i L$ is the average gain of the system and $\tau = 1.69\tau_d$ is the dynamic time of the carriers at the saturation output power. It can be observed that at low frequencies, the equation (2) simplifies to $|\Delta p_{out}| = \Delta p_{in} \bar{G} (1 + K_T)/(1 + K_T \bar{G})$ because $\omega < (1 + K_T)/\tau$ and in high frequencies $|\Delta p_{out}| = \Delta p_{in} \bar{G}$, since all the parameters K_T , \bar{G} and τ are constants.

B. Two input optical signals

A DC simulation is required to observe the XGM/XPM BW. It is primordial to launch a probe CW signal with lower optical power simultaneously with a pump modulated signal at $freq_{LO}$ with higher optical power into the SOA-circuit. The XGM is a nonlinear SOA's effect in which the pump signal modulates the carrier density and subsequently the SOA gain. Thus, the probe optical signal will be (cross) modulated by this process. In addition, the XPM is another nonlinear SOA's effect in which the pump signal modulates the refractive

index of the active region due to Kerr effect. It means that the probe signal will have a phase shift because of the change in wavelength propagation velocity owing to the new effective refractive index [14]. At the output, for simulations, just the probe modulated signal at λ_1 is transmitted and the circuit is shown in Fig. 6.

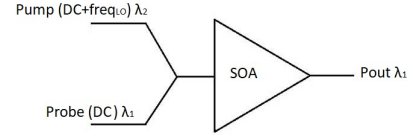


Fig. 6. Two input optical signals launched in a single SOA circuit.

In order to simulate the up-converted RF gain it is interesting to use harmonic balance parameter in the ADS. The probe signal must have the modulation part $freq_{IF}$. It is chosen to set the system order at 3 to reach until 3th harmonics and mixing order at 2 to obtain the 2nd order intermodulation. It means that ADS gives as results the: DC value, fundamental at $freq_{IF}$ and at $freq_{LO}$, four harmonics signals at $2freq_{IF}$, $3freq_{IF}$, $2freq_{LO}$, $3freq_{LO}$ and two intermodulation components at $freq_{LO}-freq_{IF}$, $freq_{LO}+freq_{IF}$. It was chosen the intermodulation components $freq_{LO}-freq_{IF}$ and $freq_{LO}+freq_{IF}$ because there is an interest of using these new RF signals produced to transmit information. The equation used to calculate the conversion gain is given by $CG = P_{out}(f_{RF}) - P_{in_2}(f_{IF})$, where $P_{out}(f_{RF})$ is the output optical power at the intermodulated frequency RF and $P_{in_2}(f_{IF})$ is the pump at Intermediate Frequency (IF).

IV. THE SOA-MZI DEVICE

The simulation circuit of the SOA-MZI device is shown in Fig. 7.

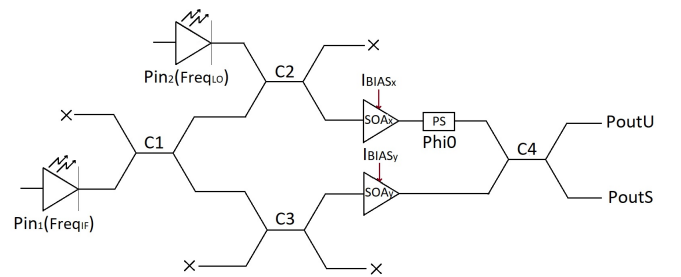


Fig. 7. The SOA-MZI schematic in the ADS.

The input optical signal P_{in_1} at a frequency f_{IF} and at a wavelength λ_1 is the data stream signal of the system also so-called “probe”. The input optical signal P_{in_2} at f_{LO} and wavelength λ_2 is the control signal also so-called “pump”. The pump signal precisely controls the phase of the system since a phase-shift occur between the 2 SOAs by generating total/partial gain due to constructive interference or loss due to destructive interference. The P_{in_1} is launched into the lower input arm of the optical coupler C1 (50:50) and is divided into equal parts for both output upper and lower arm. On the

way down, the signal is then launched on upper input arm of the coupler C3 (50:50) and go through to output upper arm to reach the lower SOA. The coupler C3 is used in case there is a need to launch a second control signal into the system to modify the phase in the lower SOA. On the way up, the signal is launched into lower input arm of the coupler C2 (50:50) and mixed with a control signal P_{in2} that is launched into upper input arm, both will be transmitted at lower output arm and reach the upper SOA. Once amplified by the upper SOA, the mixed signal will pass through a phase control device named Phase Shift (PS) to ensure the signals are in phase. At the optical coupler C4 (50:50), the amplified signal that will come out from the upper SOA will get into lower input arm to be mixed with the amplified signal from the lower SOA that will get into lower input arm. P_{outS} and P_{outU} are the switched and unswitched output power, respectively.

It is worth noting that for each optical coupler in the system, there is a phase shift of 90° between the signals crossing the arms of the couplers (lower-upper or vice-versa). This explains the system having two optical powers at the output. The P_{outS} is the optical power resulting from the maximum constructive interference generated by the 90° angle due to the coupler and P_{outU} is the optical power that undergoes destructive interference. Depending on the value of the launched optical power “control” P_{in2} , the phase will undergo a variation and the response will vary according to the phase difference between the signals.

Fig. 8 shows a DC simulation which has given the system phase characteristics.

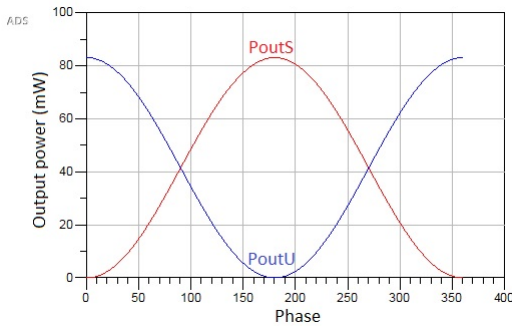


Fig. 8. Circuit simulation output phase for the SOA-MZI device.

Notice that according to the schematic in fig. 8, P_{outS} and P_{outU} have a phase-shift of 180° . A 90° phase-shift is observed every time the signal diagonally crosses the arms of the coupler, initially on coupler C1 and later on coupler C4. From that, it was simulated the output optical powers P_{outS} and P_{outU} in relation to the control optical power P_{in2} to characterize the device. Fig. 9 shows this characterization. In addition, it should be noted just in this simulation that the result generated by the ADS does not take into account the ASE noise of the system.

Fig. 9 shows the output optical power interferometer pattern as function of pump power P_{in2} . For this simulation, it was chosen the probe power $P_{in1} = -10$ dBm and $I_{BIAS} = 300$ mA. In order to simulate the maximum RF conversion gain and avoid distortion, the signal must be modulated in a linear

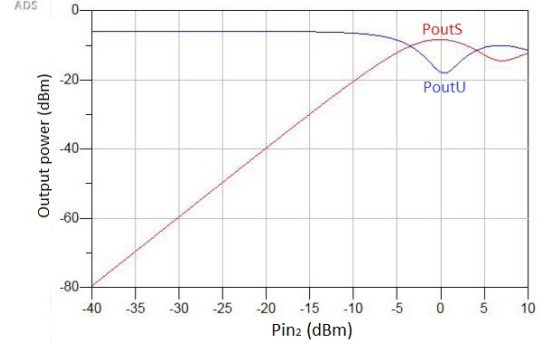


Fig. 9. SOA-MZI output optical powers at U and S as a function of pump (control) power.

shape of the curve of P_{in2} . Therefore, the maximum optical power P_{outS} must be decreased by 3 dB for each value of P_{in1} and I_{BIAS} chosen. Then, the results of simulation are shown in Fig. 10:

Operating Points for SOA-MZI given by Fig.9		
Bias current	Probe power	Pump power
mA	dBm	dBm
I=200	-20	-4.9
	-15	-4.8
	-10	-4.7
	-5	-4
	0	-1.9
I=300	-20	-4.6
	-15	-4.6
	-10	-4.5
	-5	-4
	0	-2.4
I=400	-20	-4.4
	-15	-4.4
	-10	-4.3
	-5	-3.9
	0	-2.1

Fixed Operating Points SOA-MZI	
Phi0	0°
Fif	1 GHz
FLO	20 GHz
lambda1	1550 nm
lambda2	1540 nm
m1	0.5
m2	0.5

Fig. 10. Operation points chosen for simulation the maximum RF conversion gain.

V. COMPARISON OF THE SINGLE SOA AND SOA-MZI DEVICES

With the aim of comparing both devices, both results are shown in Fig. 11 and Fig. 12. In Fig. 11 shows the XGM/XPM BW and Fig. 12 shows the up-converted RF gain of the single SOA and SOA-MZI devices. Several bias current values are taken into account.

It was noted in the simulations when using the Fig. 10 values that the bandwidth of SOA-MZI is slightly lower than the bandwidth of the single SOA. The latter fact comes from the SOA-MZI system configuration. In Fig. 7, the optical signal that has launched into the SOA is not the same one that is launched directly at the input. There are losses due to two couplers (C1 and C2). This means that P_{in1} has decreased 6 dB and P_{in2} has decreased 3 dB compared to the system with single SOA. After setting the new values of the operating points for P_{in1} and P_{in2} , the results of the XGM/XPM BW is similar for both scheme as showed in Fig. 11.

According to the Fig. 10 and the explanation above, for $I_{BIAS} = 200$ mA, the first five simulations, the BW reached

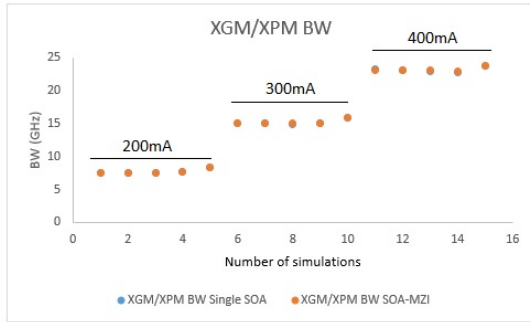


Fig. 11. XGM/XPM BW of single SOA and SOA-MZI for several bias current values.

around 7.5 GHz. For $I_{BIAS} = 300$ mA, from the sixth to tenth simulations, the BW reached around 15 GHz. And for $I_{BIAS} = 400$ mA, the last five simulations, the BW reached around 23 GHz.

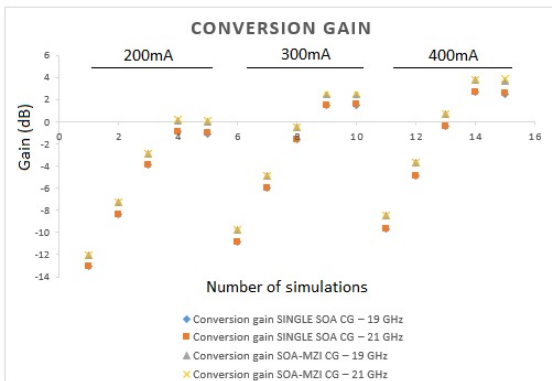


Fig. 12. Up-converted RF gain by frequency shifting for several bias current values.

Fig. 12 shows an average difference of 1 dB for SOA-MZI in comparison with the single SOA to the up-converted RF gain in the mixing orders $freq_{LO}-freq_{IF}$ and $freq_{LO}+freq_{IF}$.

Also, for the first five simulations at $I_{BIAS} = 200$ mA, the results give a conversion loss. When applied $I_{BIAS} = 300$ mA and $I_{BIAS} = 400$ mA, at lower powers, it still has a conversion loss, therefore, at higher powers, conversion gain is obtained.

VI. CONCLUSIONS

It's of great interest to researchers and telecommunications enterprises to overcome issues of the WDM systems. SOAs are, in general, a key device in MWP. Accordingly, this work aimed to introduce several simulations using SOA device. The simulation results showed the gain and the frequency response for a single input optical signal by using a single SOA scheme. Besides, it presented the SOA-MZI schematic for two input optical signals. The results of the circuit simulation output phase and output optical powers were showed. And last, but not least, a devices comparison of XGM/XPM bandwidth and RF conversion gain of both schemes were presented. According to the achieved results, it concludes that the optical

nonlinear effects of XGM/XPM bandwidth are the same for both single SOA and SOA-MZI devices parameterized by the bias current. Furthermore, the RF conversion gain for the SOA-MZI device is 1 dB on average higher than single SOA device parameterized by the bias current. It is shown that for these present purposes, the use of single SOA device instead of SOA-MZI device is more interesting due to the complexity, use of more devices, market unavailability and high cost. For the other hand, as the SOA-MZI consists in an interferometer, there are more possibilities to exploit more researches in order to improve the bandwidth system or RF conversion gain.

ACKNOWLEDGEMENTS

The author would like to acknowledge the professors at ENIB (École Nationale d'Ingénieurs de Brest) for the brilliant knowledge shared and by release the ADS license for this work. Moreover, thanks to LaCOP (Laboratório de Comunicações Ópticas) at Universidade Federal Fluminense (UFF) for complete the research.

REFERENCES

- [1] L. Lamport, *A Document Preparation System: L^AT_EX, User's Guide and Reference Manual*. Addison Wesley Publishing Company, 1986.
- [2] F. C. Silva e J. J. Sousa, "This reference is only an example," *Journal of examples*, v. 5, pp. 52–55, May 1999.
- [3] F. C. Silva e J. J. Sousa, "This reference is only an example," *Journal of examples*, v. 5, pp. 52–55, May 1999.
- [4] J. Capmany e D. Novak, "Microwave photonics combines two worlds" *Nature Photonics 1*, pp. 319 2007.
- [5] F. D. Mahad, A. S. M. Supa'at, S. M. Idrus e D. Forsyth, "Analyses of semiconductor optical amplifier (SOA) four-wave mixing (FWM) for future all-optical wavelength conversion", *Optik*, v. 124, n. 1, p. 1-3, Jan 2013
- [6] Nivedita, S. Kaur e R Goyal, "All-optical decoder/demultiplexer with enable using SOA based mach-Zehnder interferometers", *2019 6th International Conference on Signal Processing and Integrated Networks (SPIN)*, Anais...IEEE, 2019
- [7] M. Freire, E. C. Rodrigues, A. Surampudi, F. Gillet, C. Ware, A. Lavignotte e C. Lepers, "Experimental characterization of an SOA-based photonic integrated switch", *2018 Asia Communications and Photonics Conference (ACP)*, Anais...IEEE, 2018.
- [8] K. Huang, E. Wu, X. Gu, H. Pan e H. Zeng, "Ultrashort Laser Pulses for Frequency Upconversion", *In: PESHKO, I. (Ed.). Laser Pulses - Theory, Technology, and Applications*, Londres, England: InTech, 2012
- [9] W. Chen, P. Roelli, H. Hu, S. Verlekar, S. P. Amirtharaj, A. I. Barreda, T. J. Kippenberg, M. Kovylyna, E. Verhagen, A. Martínez e C. Galland, "Continuous-wave frequency upconversion with a molecular optomechanical nanocavity", *Science (New York, N.Y.)*, v. 374, n. 6572, p. 1264–1267, 2021.
- [10] P. Morel e A. Sharaiha, "Wideband time-domain transfer matrix model equivalent circuit for short pulse propagation in semiconductor optical amplifiers", *IEEE journal of quantum electronics*, v. 45, n. 2, p. 103–116, 2009.
- [11] G. Toptchiyski, S. Kindt, K. Petermann, E. Hilliger, S. Diez e H.G. Weber, "Time-domain modeling of semiconductor optical amplifiers for OTDM applications", *a joint IEEE [Journal of lightwave technology]*, v. 17, n. 12, p. 2577–2583, 1999.
- [12] I. Pierce e K. A. Shore, "Modelling pulse propagation in semiconductor optical amplifiers using wavelets", *IEE proceedings*, v. 145, n. 1, p. 88–92, 1998.
- [13] J. W. D. Chi, L. Chao e M. K. Rao, "Time-domain large-signal investigation on nonlinear interactions between an optical pulse and semiconductor waveguides", *IEEE journal of quantum electronics*, v. 37, n. 10, p. 1329–1336, 2001.
- [14] D. KASTRITSIS, "Optical sampling based on Mach-Zehnder Interferometer with Semiconductor Optical Amplifiers (SOA-MZI) for analog applications", Brest, France: ÉCOLE NATIONALE D'INGÉNIEURS DE BREST, 20 jan. 2022.